Available online at www.sciencedirect.com
ScienceDirect
ELSEVIER
Nuclear Physics A 789 (2007) 15–29
NUCLEAR PHYSICS A

Search for α decay of natural Europium

P. Belli [a], R. Bernabei [a,*], F. Cappella [b], R. Cerulli [c], C.J. Dai [d], F.A. Danevich [e], A. d'Angelo [b], A. Incicchitti [b], V.V. Kobychev [e], S.S. Nagorny [e], S. Nisi [c], F. Nozzoli [a], D. Prosperi [b], V.I. Tretyak [e], S.S. Yurchenko [e]

[a] *Dipartimento di Fisica, Università di Roma "Tor Vergata" and INFN, Sezione di Roma Tor Vergata, I-00133 Rome, Italy*
[b] *Dipartimento di Fisica, Università di Roma "La Sapienza" and INFN, Sezione di Roma, I-00185 Rome, Italy*
[c] *INFN, Laboratori Nazionali del Gran Sasso, 67010 Assergi (AQ), Italy*
[d] *IHEP, Chinese Academy, PO Box 918/3, Beijing 100039, China*
[e] *Institute for Nuclear Research, MSP, 03680 Kiev, Ukraine*

Received 27 November 2006; received in revised form 1 March 2007; accepted 5 March 2007

Available online 12 March 2007

Abstract

The indication for the α decay of ^{151}Eu ($Q_\alpha = 1.964$ MeV) with the half-life $T^\alpha_{1/2} = 5^{+11}_{-3} \times 10^{18}$ yr has been observed for the first time with the help of a low background CaF_2(Eu) crystal scintillator (mass of 370 g) in measurement at the Gran Sasso National Laboratories of the INFN during 7426 h. In a conservative approach the lower limit on the half-life of ^{151}Eu has been established as $T^\alpha_{1/2} \geqslant 1.7 \times 10^{18}$ yr at 68% C.L.

PACS: 23.60.+e; 29.40.Mc

Keywords: Alpha decay; ^{151}Eu; CaF_2(Eu) crystal scintillator; Low background experiment

1. Introduction

Two interesting observations of α activity of long-lived isotopes were recently accomplished. In fact, alpha decay of ^{209}Bi was registered with a $Bi_4Ge_3O_{12}$ scintillating bolometer; the corre-

* Corresponding author.
E-mail address: rita.bernabei@roma2.infn.it (R. Bernabei).

0375-9474/$ – see front matter
doi:10.1016/j.nuclphysa.2007.03.001

sponding half-life $T_{1/2} = (1.9 \pm 0.2) \times 10^{19}$ yr is the longest $T_{1/2}$ value for α decays observed so far [1]. Moreover, alpha decay of ^{180}W isotope with the half-life $T_{1/2} = 1.2^{+0.8}_{-0.4}(\text{stat}) \pm 0.3(\text{syst}) \times 10^{18}$ yr was observed in an experiment with $^{116}CdWO_4$ crystal scintillators [2]. The result for ^{180}W was confirmed with $CaWO_4$ crystals as scintillating low temperature bolometers ($T_{1/2} = (1.8 \pm 0.2) \times 10^{18}$ yr) [3], and as scintillator ($T_{1/2} = 1.0^{+0.7}_{-0.3} \times 10^{18}$ yr) [4].

Both natural Europium isotopes, ^{151}Eu (natural abundance $\delta = 47.81(6)\%$ [5]) and ^{153}Eu ($\delta = 52.19(6)\%$) have a positive energy release respectively to α decay and, thus, they are potentially α radioactive. Corresponding Q_α values are: $Q_\alpha = 1.964(1)$ MeV for ^{151}Eu and $Q_\alpha = 0.273(4)$ MeV for ^{153}Eu [6]. The low Q_α for ^{153}Eu gives no hope for experimental observation of its decay due to the very big expected half-life. However, for ^{151}Eu our estimations of half-life give values on the level of 10^{18} yr (see later Section 4.5), and such a sensitivity can be reached with current experimental techniques. In our knowledge, no attempts to search for this decay were previously done. In the present study a low background CaF_2(Eu) crystal scintillator was used to search for the α activity of ^{151}Eu.

2. Experiment

2.1. Detector

The low background CaF_2(Eu) scintillator (BICRON), 3" in diameter by 1" in length (mass of 370 g), doped by Europium was used in the present work. The concentration of Eu in the crystal was known from the producer as $\approx 0.5\%$ in mass. The scintillator was optically coupled by Dow Corning Q2-3067 optical couplant through 10 cm long pure quartz light guide (TETRASIL-B) to low background photomultiplier (PMT) EMI9265–B53/FL. The scintillation crystal and light guide were wrapped by PTFE reflection tape.

The detector was installed in the DAMA/R&D set-up, where it has been surrounded by Cu bricks and sealed in a low radioactive air-tight Cu box continuously flushed with high purity nitrogen gas (stored deeply underground for a long time) to avoid presence of residual environmental Radon. The Cu box has been surrounded by a passive shield made of 10 cm of high purity Cu, 15 cm of low radioactive lead, 1.5 mm of cadmium and 4 to 10 cm of polyethylene/paraffin to reduce the external background. The whole shield has been closed inside a Plexiglas box, also continuously flushed by high purity nitrogen gas.

An event-by-event data acquisition system records amplitude and arrival time of events. Moreover, the signals from the PMT were also recorded by a 160 MSa/s Transient Digitizer over a time window of 3125 ns.

The experiment had been carried out in the underground Gran Sasso National Laboratories of the INFN at a depth of 3600 m w.e.

2.2. Response of the CaF_2(Eu) detector to γ quanta and α particles

The energy scale and resolution of the CaF_2(Eu) detector for γ quanta was measured with ^{22}Na, ^{133}Ba, ^{137}Cs, ^{228}Th and ^{241}Am sources. For instance, the energy resolution was 28%, 11.4% and 7.5% for γ lines 60 keV (^{241}Am), 356 keV (^{133}Ba) and 662 keV (^{137}Cs), respectively. The energy dependence of the energy resolution can be fitted by the function: $\text{FWHM}_\gamma\ (\text{keV}) = \sqrt{3.7(4) \cdot E_\gamma}$, where E_γ is the energy of γ quanta in keV.

The response of the detector to α particles was studied with a collimated ^{241}Am α source. The dimensions of the collimator made of teflon are $\oslash 0.75 \times 2$ mm. By using different sets of

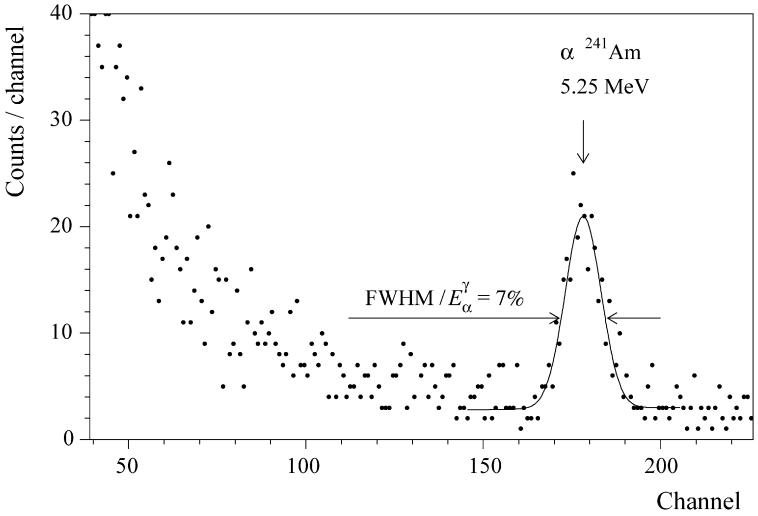

Fig. 1. Energy spectrum of ^{241}Am α particles measured by the CaF_2(Eu) scintillation detector. E_α^γ is energy of α particles in γ scale of the detector.

absorbers (mylar film 0.65 mg/cm^2 of thickness; and a few mm layer of air in some cases), α particles with energies of 1.00, 1.30, 1.45, 1.59, 2.27, 3.23, 3.98, 4.66 and 5.25 MeV were obtained, which allows us to calibrate the CaF_2(Eu) detector in the energy range of interest. The energies of α particles after passing the collimator and absorbers were calculated with the help of the GEANT4 package [7]. Furthermore these energies were measured with the help of a surface-barrier semiconductor detector. The energy spectrum of ^{241}Am α particles (energy of α particles after passing through the collimator was calculated as 5.25 MeV) is presented on Fig. 1.

The energy resolution for α particles (FWHM$_\alpha/E_\alpha^\gamma = 7\%$, where E_α^γ is energy of α particles in γ scale) was roughly similar to that for γ quanta. Specific α's energies in the energy interval 1–5.25 MeV were obtained with the set of calibrated absorbers. In addition, the α peaks of ^{147}Sm, ^{232}Th and ^{238}U observed in the background spectrum (see Section 3.2), as well as the data of the time-amplitude analysis (^{215}Po, ^{216}Po, ^{219}Rn, ^{220}Rn, ^{224}Ra, Section 3.1) and pulse-shape analysis of double pulses (^{212}Po, ^{214}Po, Section 3.3) were used to extend energy of α particles up to 8.8 MeV.

The dependence of the α/β ratio (i.e. ratio of energy of α particle measured in γ scale by scintillator to its real energy) versus the energy of α particles is shown on Fig. 2.

For the energies above ≈ 2 MeV, the dependence of α/β ratio on energy can be described as: $\alpha/\beta(E_\alpha) = 0.092(4) + 0.0168(7)E_\alpha$, where E_α is the energy of α particles in MeV. It gives the value of the α/β ratio of 0.124(4) at the energy of α decay of ^{151}Eu ($E_\alpha = 1.912$ MeV), which leads to 238(8) keV in γ scale. However, one has to take into account the measured non-linear behaviour of the α/β ratio near the energy of 2 MeV.[1] To describe the behaviour of the α/β ratio

[1] Because quenching of the scintillation light caused by α particles (in comparison with electrons) is due to the higher ionization density of α particles [8], such a behaviour of the α/β ratio can be explained by the energy dependence of the ionization density of α particles. Increasing of α/β ratio at energies of α particles lower than 1.5–2 MeV was observed for $CdWO_4$ [2], and $CaWO_4$ [9] scintillators. Similar behaviour of α/β ratio was measured very precisely for CsI(Tl) scintillator [10].

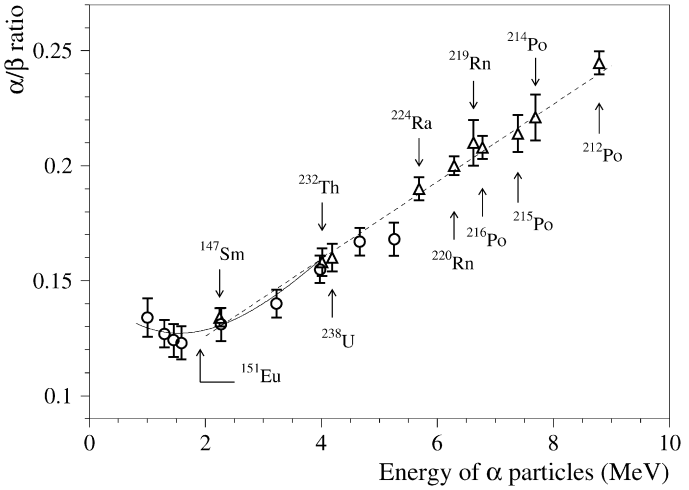

Fig. 2. The energy dependence of the α/β ratio for the CaF_2(Eu) scintillation detector. The points measured with ^{241}Am source are shown by circles. The peaks of ^{147}Sm and ^{232}Th were obtained by the pulse-shape discrimination of the background data. The points corresponding to the α peaks of ^{224}Ra, ^{220}Rn, ^{219}Rn, ^{216}Po, ^{215}Po were selected with the help of the time-amplitude analysis; peaks of ^{212}Po and ^{214}Po were obtained by the pulse-shape analysis of the double events in the background data. Linear fit of the data in the energy interval 2–9 MeV is shown by the dashed line. Solid line represents the fitting curve of the experimental points at low energies.

in the vicinity of the expected ^{151}Eu α peak, the data were fitted by polynomial function in the energy interval of α particles 1–4 MeV. According to the fit, $\alpha/\beta = 0.128(19)$ at the energy of ^{151}Eu α particles, i.e. the expected energy of ^{151}Eu α peak in gamma scale is 245(36) keV.[2]

2.3. *Mass-spectrometry of the CaF_2(Eu) crystal*

The concentration of Eu in the CaF_2(Eu) crystal was determined with the help of the Inductively Coupled Plasma–Mass Spectrometry analysis (ICP-MS, Agilent Technologies model 7500a). A representative part of the CaF_2(Eu) crystal has been reduced to powder by mechanical treatment inside a cleaned polyethylene bag to avoid possible contamination. To measure Eu concentration in a CaF_2 crystal, one should overcome two problems. At first, Calcium fluoride is rather insoluble in acids. The second problem could appear due to formation of insoluble EuF_3 during dissolving procedure. Several tests applying different solutions (HCl, HNO_3, H_2SO_4, H_2O_2, NH_4, and their mixtures) have been carried out to obtain maximum solubility of CaF_2(Eu) crystal. The best solutions were as following: (a) H_2SO_4 95%; (b) mixture of 2 parts of HCl and 5 parts of HNO_3. Solubility of CaF_2 was about 75% and 65%, respectively. To estimate the efficiency of Eu recovery, a sample of spike Eu was added to the solution (b). 98% of the spiked Eu was measured in the final solution. Therefore the effect of insoluble EuF_3 formation is neg-

[2] There is contribution to scintillation light from recoiling nuclei associated with the internal α decays; however, it is small. For instance, the energy of recoil in ^{232}Th decay is 70 keV. Supposing, very conservatively, that quenching for the recoil nuclei is equal to quenching for Calcium recoils reported in [11] (≈ 17), one can get estimation of ≈ 4 keV for the signal from the recoil. It leads to changing of the alpha/beta ratio for ^{232}Th α's to 0.159 instead of 0.158(6). However, the real scintillation from the recoil (^{228}Ra) is expected to be even smaller. Therefore, one can ignore the effect of the recoils for CaF_2(Eu) scintillator.

ligible. Six solutions were prepared and measured by ICP-MS analysis, three of (b), and other three of (a) type. Concentration of Eu in the CaF_2(Eu) crystal determined as average of the six measurements carried out by standard addition method is equal to $(0.4 \pm 0.1)\%$; the uncertainty on the measurement is relative high because it also takes into account the uncertainty on the sample preparation procedure. The concentration of Eu in the CaF_2(Eu) crystal is in agreement with that known from the producer of the scintillator. The contaminations by Nd, Sm, Gd, Hf, Os, Pt, Bi, Th, U (all these elements have α active isotopes) were also measured by the ICP-MS. Only limits on the level of < 0.1 ppm were obtained for all of them.

2.4. Low background measurements

The energy scale of the CaF_2(Eu) detector was measured in the beginning of the measurements, and then was checked twice: in the middle and in the end of the low background experiment. Both the energy scale and the energy resolution were reasonably stable with deviations in the range of 2–3%. Additionally, the energy scale was controlled by analysis of position of γ and α peaks present in the background. A remained shift of the gain was corrected by the off-line analysis. By using the calibration and background data, we found that the energy resolution for γ quanta in the final spectrum measured during 7426 h after the off-line correction can be described by the function $\mathrm{FWHM}_\gamma\ (\mathrm{keV}) = \sqrt{4.0(4) \cdot E_\gamma}$, where E_γ is the energy of γ quanta in keV. The energy spectrum accumulated in the low background set-up with the CaF_2(Eu) detector is presented in Fig. 3.

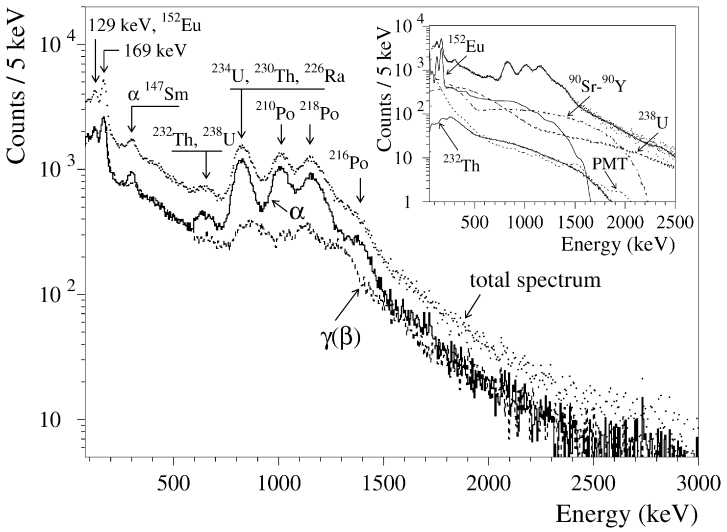

Fig. 3. The energy spectrum of the CaF_2(Eu) scintillator measured during 7426 h in the low background set-up (points). The spectra, obtained by applying the pulse-shape discrimination technique (see text), are shown by dashed line for $\gamma(\beta)$ component and solid line for α component. The peaks with energies of 129 keV and 169 keV are due to presence of ^{152}Eu in the crystal. The peak at the energy ≈300 keV corresponds to α active ^{147}Sm. The group of peaks in the energy region 0.6–1.5 MeV is due to internal contamination of the crystal by α active daughters of ^{232}Th and ^{238}U. (Inset) Fit of the total spectrum by simulated models (see Section 4.1) in 90–2200 keV energy interval is shown by solid line. Also shown are the most important components of $\gamma(\beta)$ background: spectra of ^{152}Eu, ^{90}Sr–^{90}Y, β active daughters of ^{232}Th and ^{238}U, and model distribution of external γ's from PMT.

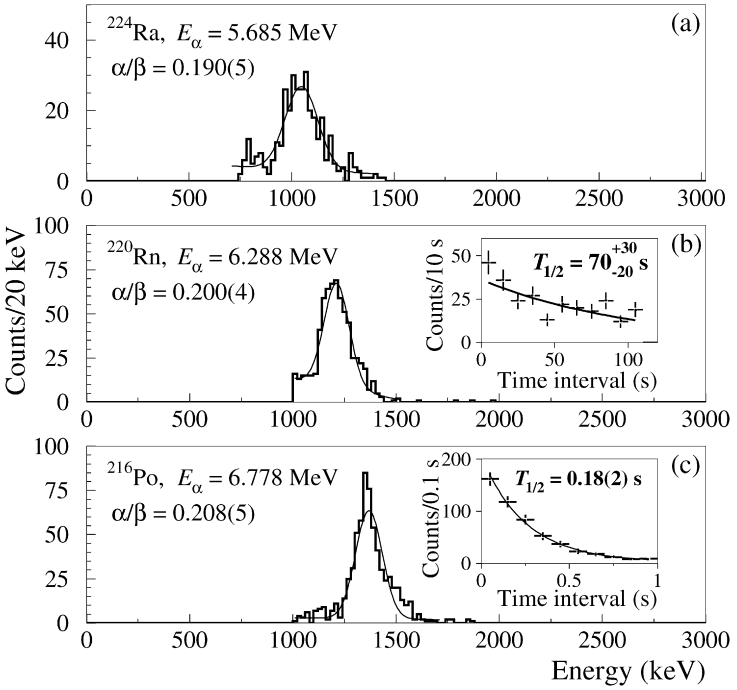

Fig. 4. Alpha peaks of ^{224}Ra, ^{220}Rn and ^{216}Po selected by the time-amplitude analysis from the data accumulated during 7426 h with the CaF_2(Eu) detector. The obtained half-lives of ^{220}Rn (70^{+30}_{-20} s) and ^{216}Po (0.18 ± 0.02 s) are in agreement with the table values (55.6 s and 0.145 s, respectively [15]).

3. Data analysis

3.1. Time-amplitude analysis

The raw data of the low background measurements with the CaF_2(Eu) crystal were analyzed by the time-amplitude method, when the arrival time and energy of each event were used for the selection of fast decay chains in ^{232}Th and ^{235}U families.[3] To estimate the activity of ^{228}Th (the ^{232}Th family) the following sequence of α decays was searched for and observed: ^{224}Ra ($Q_\alpha = 5.789$ MeV, $T_{1/2} = 3.66$ d) $\rightarrow$ ^{220}Rn ($Q_\alpha = 6.405$ MeV, $T_{1/2} = 55.6$ s) $\rightarrow$ ^{216}Po ($Q_\alpha = 6.907$ MeV, $T_{1/2} = 0.145$ s) $\rightarrow$ ^{212}Pb. The obtained α peaks (see Fig. 4) as well as the distributions of the time intervals between events are in a good agreement with those expected for α particles of the ^{224}Ra $\rightarrow$ ^{220}Rn $\rightarrow$ ^{216}Po $\rightarrow$ ^{212}Pb chain. On this basis the activity of ^{228}Th in the CaF_2(Eu) crystal was calculated as 0.134(17) mBq/kg.

The same technique was applied to select decays of chain ^{223}Ra ($Q_\alpha = 5.98$ MeV, $T_{1/2} = 11.44$ d) $\rightarrow$ ^{219}Rn ($Q_\alpha = 6.95$ MeV, $T_{1/2} = 3.96$ s) $\rightarrow$ ^{215}Po ($Q_\alpha = 7.526$ MeV, $T_{1/2} = 1.78$ ms) $\rightarrow$ ^{211}Pb from the ^{235}U family. Corresponding activity of ^{227}Ac in the crystal was estimated as 0.011(7) mBq/kg.

[3] The technique of the time-amplitude analysis is described in detail in [12–14].

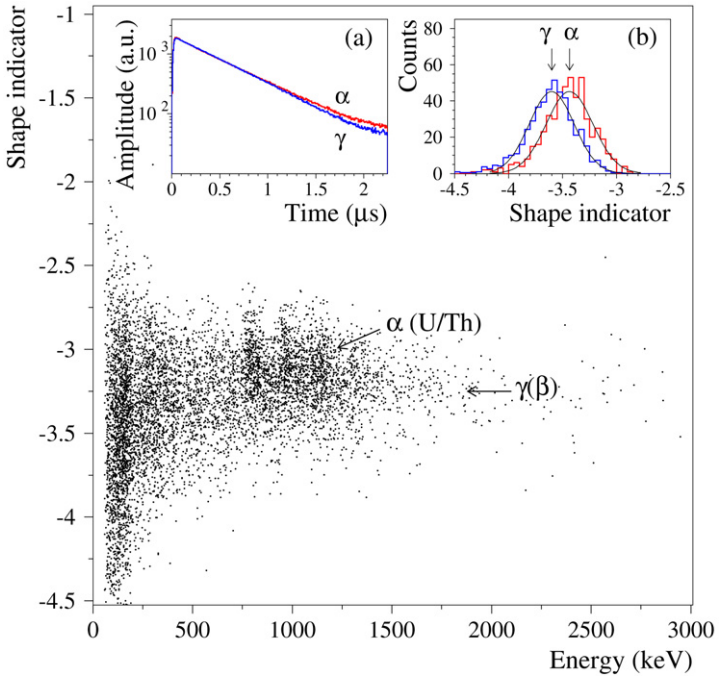

Fig. 5. Distribution of shape indicator (see text) versus energy for the background events accumulated during 144 h of exposition with the CaF_2(Eu) detector. The population of α events belonging to the U/Th families is slightly separated from the $\gamma(\beta)$ background. The pulse shapes of the CaF_2(Eu) scintillator for α particles and γ rays are shown in inset (a). The distributions of shape indicator measured with the CaF_2(Eu) scintillation detector for α particles (≈ 4 MeV) and γ quanta (≈ 0.6 MeV) are shown in inset (b).

3.2. Pulse-shape discrimination

The calibration measurements with α (^{241}Am) and γ (^{60}Co) sources were carried out to check a possibility of pulse-shape discrimination between α and $\gamma(\beta)$ events in the CaF_2(Eu) scintillator. The time characteristics of CaF_2(Eu) scintillator were studied with the help of a Transient Digitizer operated at the sample rate of 160 MSa/s. The pulse shapes for γ quanta and α particles measured with the CaF_2(Eu) crystal are depicted in inset (a) of Fig. 5.

The pulse shapes can be fitted by sum of exponential functions: $f(t) = \sum A_i(e^{-t/\tau_i} - e^{-t/\tau_0})/(\tau_i - \tau_0)$, $t > 0$, where A_i are intensities, τ_i are decay constants for different light emission components and τ_0 is integration constant of electronics. Two components of scintillation light with $\tau_1 \approx 0.5$ μs and $\tau_2 \approx 6$–8 μs were obtained from the fit. The intensities of the components are $A_1 = 79\%$, $A_2 = 21\%$ for α particles and $A_1 = 93\%$, $A_2 = 7\%$ for γ quanta.

This difference allows to discriminate events from α decays inside the crystal from the $\gamma(\beta)$ background. We applied for this purpose the optimal filter method proposed in [16] and already realized with $CdWO_4$ scintillators in [17] (see also [18] and references therein). This method was successfully used for pulse-shape discrimination in different scintillators: CeF_3 [14], $CaWO_4$ [9], YAG:Nd [19], $ZnWO_4$ [20] and $PbWO_4$ [21].

To obtain a numerical parameter of CaF_2(Eu) signal, the so-called shape indicator (SI), the following formula was applied for each pulse: $SI = \sum f(t_k)P(t_k)/\sum f(t_k)$, where the sum is over time channels k, starting from the origin of the pulse up to 2.25 μs, $f(t_k)$ is the digitized

amplitude (at the time t_k) of a given signal. The weight function $P(t)$ is defined as: $P(t) = \{f_\alpha(t) - f_\gamma(t)\}/\{f_\alpha(t) + f_\gamma(t)\}$, where $f_\alpha(t)$ and $f_\gamma(t)$ are the reference pulse shapes for α particles and γ quanta which were obtained by summing up big number of α and γ events. An indication for discrimination between α particles and γ quanta was achieved as one can see in inset (b) of Fig. 5 where the shape indicator distributions measured by the CaF_2(Eu) scintillation crystal with α particles ($E_\alpha \approx 4$ MeV) and γ quanta ($E_\gamma \approx 0.6$ MeV) are shown. The scatter plot of the shape indicator versus energy (Fig. 5) demonstrates some pulse-shape discrimination ability for the background data accumulated with CaF_2(Eu) scintillator.

The energy dependence of the shape indicators and standard deviations (as one can see in Fig. 5(b) the distributions of the shape indicator are well fitted by a Gaussian function) for γ rays (^{137}Cs, ^{22}Na, ^{60}Co) and α particles (^{241}Am α source) was measured in the calibration measurements.

Despite a rather low discrimination, this method allows to check the nature of the events in the background spectrum (Fig. 3). For this purpose the data were separated in two parts. The first one has been selected with condition $SI < SI_\gamma$; it contains 50% of $\gamma(\beta)$ events ("$\gamma(\beta)$" spectrum). The second part ("α") was selected with condition $SI > SI_\gamma$. This spectrum also contains 50% of $\gamma(\beta)$ events while the number of α events is larger than that in the "$\gamma(\beta)$" distribution. Both spectra are presented in Fig. 3. There is a visible difference between the spectra. As it will be

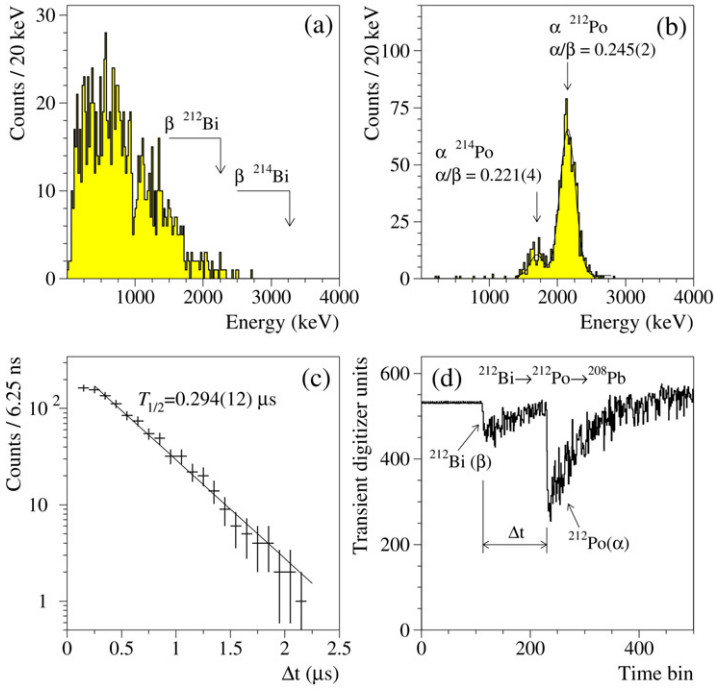

Fig. 6. The energy (a,b) and time (c) distributions for fast sequence of β (^{212}Bi) and α (^{212}Po) decays selected by the pulse-shape analysis from the background data recorded over 7426 h. Fit of the time distribution gives half-life $T_{1/2} = (0.294 \pm 0.012)$ μs which is in good agreement with table value for ^{212}Po (0.299 μs [15]). (d) Example of such an event in the CaF_2(Eu) scintillator. The peak with energy $\simeq 1.7$ MeV (b) corresponds to α decay of ^{214}Po following after β decay of ^{214}Bi. Note that this peak is depressed by a factor ≈ 110 because of the used Transient Digitizer time window, which allows to record 74% of the $^{212}\text{Bi} \rightarrow {}^{212}\text{Po}$ events and only 0.9% of $^{214}\text{Bi} \rightarrow {}^{214}\text{Po}$ events.

demonstrated below (Section 4.1), pulse-shape discrimination allows to identify α active nuclides present in the crystal.

3.3. Pulse-shape analysis of double pulses

In addition, the method to select double pulses produced by fast chains of decays of ^{212}Bi ($Q_\beta = 2.254$ MeV) $\rightarrow$ ^{212}Po ($Q_\alpha = 8.954$ MeV, $T_{1/2} = 0.299$ μs) $\rightarrow$ ^{208}Pb (^{232}Th family) and ^{214}Bi ($Q_\beta = 3.272$ MeV) $\rightarrow$ ^{214}Po ($Q_\alpha = 7.833$ MeV, $T_{1/2} = 164$ μs) $\rightarrow$ ^{210}Pb (^{238}U) in the CaF_2(Eu) scintillator was developed. The result of this analysis is presented in Fig. 6.

The obtained spectra lead to the ^{226}Ra activity in the CaF_2(Eu) crystal of 1.3(2) mBq/kg. The activity of ^{212}Po (which is in equilibrium with ^{228}Th) was calculated as 0.124(5) mBq/kg. This value is in agreement with the result of the time-amplitude analysis.

4. Results and discussion

4.1. Simulation of the background spectrum

Activities of α active nuclides present in the CaF_2(Eu) scintillator as trace contaminations were estimated by analysis of α peaks, determined with the help of the pulse-shape discrimination (Fig. 3). The peak with the energy (303 ± 3) keV can be explained by ^{147}Sm activity in the crystal at the level of 0.34(4) mBq/kg. This activity corresponds to Sm contamination in the crystal at the level of 3 ppb, which is much lower than that of sensitivity of the mass spectrometry analysis. The α peak at the energy ≈ 660 keV belongs to ^{232}Th and ^{238}U with the activities 0.05(1) and 0.06(1) mBq/kg, respectively. The activity of ^{232}Th is smaller than that of ^{228}Th due to broken equilibrium of ^{232}Th family. The group of α peaks at the energy 0.8–1.4 MeV is due to α active nuclides of U/Th. The model to describe the peaks was built taking into account the α/β ratio and possible broken equilibrium of the families. The fit of the background spectrum by the model gives the total activity of U/Th nuclides in the crystal at the level of 8(2) mBq/kg. The measured activities of α active U/Th daughters in the CaF_2(Eu) crystal scintillator (or limits on their values) are given in Table 1. To take into account presence in the crystal of β active isotopes (from U/Th families, ^{40}K, ^{60}Co, ^{90}Sr–^{90}Y, ^{137}Cs, ^{154}Eu) and external γ rays, the measured background spectrum of the CaF_2(Eu) detector was simulated with the GEANT4 package [7]. Initial kinematics of particles emitted in β decays of nuclei was generated with the DECAY0 event generator [22]. In the low energy part of the spectrum the background is caused mainly by β decay of ^{152}Eu.[4] Corresponding activity of ^{152}Eu in the crystal was estimated as 10(2) mBq/kg. There are no other clear peculiarities in the spectrum which could be referred to the internal trace contamination by radioactive nuclides. Limits on activities of ^{40}K, ^{60}Co, ^{90}Sr–^{90}Y, ^{137}Cs, ^{154}Eu, ^{228}Ac (daughter of ^{228}Ra from the ^{232}Th family) were set on the basis of the experimental data. With this aim the spectrum was fitted in different energy intervals by the model, which includes the simulated distributions of ^{152}Eu, of U/Th daughters, an exponential function to describe external γ background and the components searched for. The fitting curve and main components of the background are presented in Fig. 3 (inset).

The summary of the measured radioactive contamination of the CaF_2(Eu) crystal scintillator (or limits on their activities) is given in Table 1.

[4] Nuclei of ^{152}Eu ($T_{1/2} = 13.5$ yr) were created in result of neutron captures by natural ^{151}Eu.

Table 1
Radioactive contamination of the CaF_2(Eu) scintillator. Activities are in mBq/kg

Chain	Nuclide	Activity
^{232}Th	^{232}Th	0.05(1)
	^{228}Ra	$\leqslant 0.6$
	^{228}Th	0.13(2)
^{235}U	^{227}Ac	0.011(7)
^{238}U	^{238}U	0.06(1)
	^{226}Ra	1.3(2)
	^{210}Po	0.9(2)
Total U/Th α activity		8(2)
	^{40}K	$\leqslant 7$
	^{60}Co	$\leqslant 3$
	^{90}Sr–^{90}Y	$\leqslant 4$
	^{137}Cs	$\leqslant 0.3$
	^{147}Sm	0.34(4)
	^{152}Eu	10(2)
	^{154}Eu	$\leqslant 0.5$

4.2. α Decay of ^{151}Eu to the ground state of ^{147}Pm

The low energy part of the background spectrum measured with the CaF_2(Eu) crystal scintillator in the low background set-up during 7426 h is shown in Fig. 7. There is a peculiarity in the spectrum at the energy near 250 keV—in agreement with the expected energy of peak of the ^{151}Eu alpha decay—which gives an indication on existence of this process. To estimate half-life of ^{151}Eu, the background energy spectrum was fitted by simple model consisting of two Gaussian peaks (related with α decay of ^{151}Eu and ^{147}Sm) and exponential function to describe background. The fit was performed in the energy region with starting point from 215 keV to 230 keV (with step of 5 keV) and with final point from 340 keV to 410 keV. In the most of the intervals the fit gives positive effect at the level of 1.2–2.8σ. The best fit (χ^2/n.d.f. = 0.42), achieved in the interval 225–365 keV (see Fig. 7), gives for the area of the expected peak $S = (302 \pm 232)$ counts. With these values, using the Feldman–Cousins procedure [23], one can conclude that observation of the effect is statistically significant and amplitude of the effect is inside the interval [5, 682] counts with 90% C.L. (or [98, 534] counts with 68% C.L.). The energy of the peak is (255 ± 7) keV. It corresponds to the energy of α particles (1.98 ± 0.04) MeV, in agreement with the expected value of 1.912 MeV for α's of ^{151}Eu. In accordance with the ICP-MS measurements, the CaF_2(Eu) crystal contains $2.8(7) \times 10^{21}$ nuclei of ^{151}Eu. Thus, the half-life of ^{151}Eu is as the following: $T_{1/2} = 5.4^{+11.4}_{-2.4}(\text{stat}) \pm 1.4(\text{syst}) \times 10^{18}$ yr. The systematic error, which is much lower than statistical, is related mainly with the uncertainty of the number of Eu nuclei in the crystal and with variation of the peak's area depending on the interval of the fit.

The pulse-shape discrimination analysis was used to clarify the nature of events in the ≈ 250 keV peak. As one can see on the bottom curve of Fig. 7, while this effect is present in the α component of the spectrum, there is no evidence for this peak in the $\gamma(\beta)$ component. Fit of the α spectrum in the energy interval 225–365 keV by the same model (two peaks plus exponential function) gives for the area of the ^{151}Eu α peak: (254 ± 224) counts and for the energy: $E_\alpha = (1.96 \pm 0.03)$ MeV. The α spectrum contains 68% of α events (the efficiency was

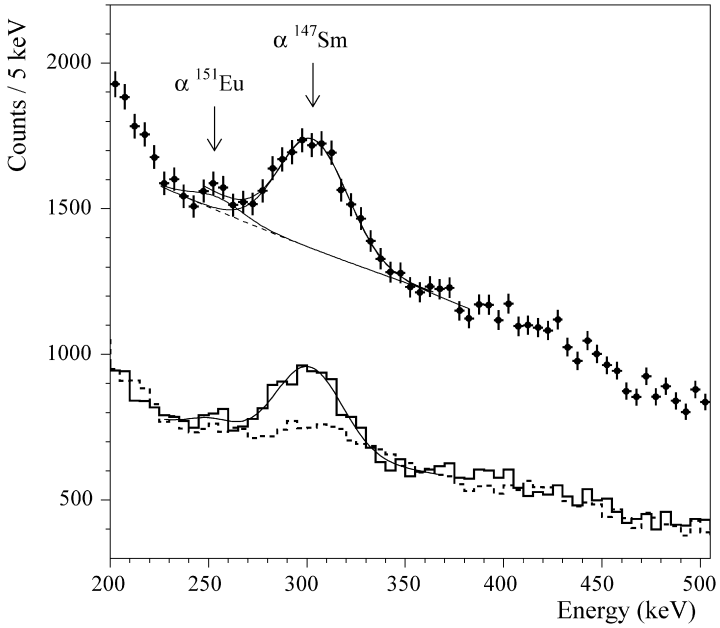

Fig. 7. *Top*: low energy part of the background spectrum measured during 7426 h in the low background set-up with the CaF_2(Eu) scintillator. The peculiarity on the left of the ^{147}Sm peak can be attributed to the α decay of ^{151}Eu with the half-life $T_{1/2} = 5 \times 10^{18}$ yr. *Bottom*: the spectra obtained by applying the pulse-shape discrimination technique are shown by dashed ($\gamma(\beta)$ component) and solid (α component) lines.

estimated by using the α peak of ^{147}Sm) and so, the total area of the peak is (374 ± 329) counts, in agreement with the result obtained by fitting of the total background spectrum. This gives the value of the half-life: $T_{1/2} = 4.4^{+11.3}_{-2.1}(\text{stat}) \times 10^{18}$ yr at 68% C.L.

Finally, we give the following estimation of the half-life of ^{151}Eu relatively to the α decay to the ground state of ^{147}Pm:

$$T^{\alpha}_{1/2}(g.s. \to g.s.) = 5^{+11}_{-3} \times 10^{18} \text{ yr}.$$

Because of rather big statistical uncertainty of this result, one can use also more conservative approach and estimate only an upper limit on half-life of ^{151}Eu. By analysis of the fits of the measured spectrum, we have obtained the following limit on the half-life of ^{151}Eu:

$$T^{\alpha}_{1/2}(g.s. \to g.s.) \geqslant 1.7 \times 10^{18} \text{ yr at 68\% C.L.}$$

There are several α decaying nuclides with energy releases close to the ^{151}Eu value of $Q_\alpha = 1.964(1)$ MeV. These are: ^{144}Nd ($Q_\alpha = 1.905(2)$ MeV [6]), ^{148}Sm (1.986(1) MeV) and ^{152}Gd (2.203(1) MeV); all other alpha decayers have Q_α values bigger than that of ^{147}Sm which is present in the background spectrum as peak at ≈300 keV. ^{148}Sm has near the same abundance ($\delta = 11.2\%$ [5]) as ^{147}Sm (15.0%); however, because of its big half-life (7×10^{15} yr in comparison with 1.06×10^{11} yr for ^{147}Sm), peak of ^{148}Sm should be near five orders of magnitude lower than peak of ^{147}Sm and, thus, cannot mimic alpha decay of ^{151}Eu. Contaminations of the CaF_2(Eu) crystal by Nd and Gd are lower than 0.1 ppm that is known from the ICP-MS analysis. With $T_{1/2} = 2.29 \times 10^{15}$ yr and $\delta = 23.8\%$, ^{144}Nd could contribute not more than 10 events in the ^{151}Eu peak. Contribution of ^{152}Gd ($T_{1/2} = 1.08 \times 10^{14}$ yr and $\delta = 0.2\%$) should be even lower.

Thus, the observed alpha peak at ≈ 250 keV cannot be mimicked by some other α decaying nuclides present in the CaF_2(Eu) crystal.

4.3. Limit on α decay of ^{151}Eu to the first excited level of ^{147}Pm

In addition to decay of ^{151}Eu to the ^{147}Pm ground state, also the first excited level of ^{147}Pm ($5/2^+$, $E_{\rm exc} = 91$ keV) can be populated[5]; corresponding Q_α value is 1.873 MeV. Energy of α particles is $E_\alpha = 1.823$ MeV what, taking into account the α/β ratio, corresponds to energy of 234 keV in the γ scale of the CaF_2(Eu) detector. In a subsequent deexcitation process of the excited ^{147}Pm level, some particles will be emitted: or single gamma quantum ($E_\gamma = 91$ keV) with probability of 33%, or conversion electron plus cascade of X rays and Auger electrons with probability 67% (coefficient of conversion for this transition is equal to 2.06 [24]). Because all these low-energy particles are effectively absorbed inside the crystal, the full energy observed by the CaF_2(Eu) detector will be equal to (325 ± 33) keV. Peak with this energy, which should be on the right slope of the ^{147}Sm peak, is not evident in the experimental data (see Fig. 7). Fit of the background spectrum by a model consisting of two peaks (^{147}Sm and the peak searched for) plus an exponential function gives the following upper limit on α decay of ^{151}Eu to the first excited level of ^{147}Pm:

$$T^{\alpha}_{1/2}\big(g.s. \to 5/2^+\big) \geqslant 6 \times 10^{17} \text{ yr at 68\% C.L.}$$

This limit is one order of magnitude higher than that reported in work [25] where γ quanta with the energy 91 keV were searched for from a sample of $Li_6Eu(BO_3)_3$ crystal; these measurements were performed with the help of an ultra-low background HP Ge γ spectrometer (volume of 408 cm^3) in the Gran Sasso National Laboratories.

4.4. About presence of Promethium in the Earth crust

Promethium is one of the rarest elements abundant on the Earth in extremely small quantities. All known 38 isotopes of Promethium are unstable and only 5 have noticeable half-lives in the range from 0.7 to 17.7 yr [26]. Thus, it could be present on the Earth only as a temporal product created in U/Th fission, cosmogenic reactions induced by cosmic rays, radioactive decays, and neutron captures on other nuclides. Predominantly it is created in spontaneous fission (SF) of ^{238}U, where isotopes with $A = 147$ are born with yields of 1.88% (^{147}Ba), 2.32% (^{147}La) and 0.20% (^{147}Ce) [27], via subsequent chain of radioactive decays $^{147}\text{Ba} \to {}^{147}\text{La} \to {}^{147}\text{Ce} \to \cdots \to {}^{147}\text{Pm}$. The overall yield of ^{147}Pm per SF of ^{238}U, created in this way, is thus 4.4%, in accordance with older measurements [28], where only the ^{147}Pm activity in U ore was found as $3(1) \times 10^{-4}$ Bq per 1 g of U (this corresponds to 4.5(1.5)% yield per SF of ^{238}U). Taking into account the Uranium abundance in the Earth crust 2.7×10^{-4}% and the mass of the crust 2.36×10^{22} kg [29], one can calculate that equilibrium mass of natural Pm in the Earth crust is equal to 560 g. This amount is extremally small but it is higher than the equilibrium natural abundance of radiogenic Francium (350 g, family of ^{235}U) and Astatine (0.13 g in decays of ^{238}U chain and 0.06 g in ^{235}U decays).

The observed α decay of ^{151}Eu opens additional source of natural Promethium in the Earth crust, however, lower than that generated by the Uranium SF. Taking into account the abun-

[5] Higher ^{147}Pm levels could be populated too; however, because of the exponential dependence on energy release, probabilities for such α decays are much lower.

Table 2
Theoretical calculations of half-lives for α decay $^{151}\mathrm{Eu} \to {}^{147}\mathrm{Pm}$

Populated level	Theoretical $T_{1/2}$, yr				
	Calculated here on the basis of Refs. [30–33]				Calculated in
	[30]	[31]	[32]	[33]	[35]
Ground state	3.0×10^{17}	3.6×10^{18}	6.3×10^{17}	5.9×10^{17}	1.6×10^{18}
$5/2^+$, 91 keV	7.7×10^{18}	1.0×10^{20}	1.5×10^{19}	1.7×10^{19}	–

dance of Europium in the crust (2×10^{-4}%), one can estimate the equilibrium concentration of $0.2^{+0.4}_{-0.1}$ ng of Promethium per 1 kton of natural Europium and the total amount of Promethium born by ^{151}Eu in the whole Earth crust as: 12^{+17}_{-8} g.

4.5. Comparison with theory

Theoretical half-life value for ^{151}Eu was calculated with the cluster model of Ref. [30] and with semiempirical formulae [31,32] based on liquid drop model and description of α decay as a very asymmetric fission process. Approaches [30–32] were tested with a set of experimental half-lives of almost four hundred α emitters and demonstrated good agreement between calculated and experimental $T_{1/2}$ values, mainly inside the factor of 2–3. The parametrization of Ref. [33] was also used where free parameters in formula for $T_{1/2}$ were found by fitting experimental half-lives in the rare-earth mass region, of interest in the present paper. Because of the difference between spins of the ground state of parent ^{151}Eu nucleus ($5/2^+$) and the ground state of ^{147}Pm ($7/2^+$), the emitted α particle will have non-zero angular momentum: values of $L = 2, 4, 6$ are allowed by the selection rules. Thus, in $T_{1/2}$ estimation, we take into account the hindrance factor of 2.163, calculated in accordance with [34] for the most preferable value of $L = 2$. In α decay to the first excited level of ^{147}Pm ($5/2^+ \to 5/2^+$ transition), values of $L = 0, 2, 4$ are possible with the most preferable $L = 0$ which supposes no additional hindrance factor. The results of calculations are given in Table 2 together with the $T_{1/2}$ value determined in Ref. [35]; all the values are inside the range of $(0.3–3.6) \times 10^{18}$ yr. The half-life of ^{151}Eu, measured in this experiment, is in agreement with theoretical calculations with the help of semiempirical method [31] and with the value determined in [35]. Agreement with other theoretical works [30,32,33] is worse.

Calculated $T_{1/2}$ estimations for α decay of ^{151}Eu to the first excited level of ^{147}Pm are on the level of 10^{19}–10^{20} yr (see Table 2). The upper limit set in our experiment for this decay is still below these theoretical expectations.

5. Conclusions

Alpha activity of natural Europium isotope ^{151}Eu was searched for with the help of a low background CaF_2(Eu) crystal scintillator in the Gran Sasso National Laboratories of the INFN. The response of the CaF_2(Eu) detector to α particles was studied in wide energy interval of 1–9 MeV. Some pulse-shape discrimination between α particles and γ quanta was demonstrated. Background and radioactive contaminations of the CaF_2(Eu) crystal were measured.

The indication for the α decay of ^{151}Eu with the half-life $T^{\alpha}_{1/2} = 5^{+11}_{-3} \times 10^{18}$ yr has been observed for the first time. In a conservative approach the lower limit on half-life of ^{151}Eu has been established as $T^{\alpha}_{1/2} \geqslant 1.7 \times 10^{18}$ yr at 68% C.L. In addition, the lower limit $T^{\alpha}_{1/2} \geqslant 6 \times 10^{17}$ yr

at 68% C.L. was set for the α transition to the first excited level of ^{147}Pm. Measured value of half-life of ^{151}Eu is in agreement with theoretical calculations based on the liquid drop model and description of α decay as a very asymmetric fission process [31,35]. Consistency with $T_{1/2}$ predictions based on other approaches or parametrizations is worse.

It should be noted one interesting outcome obtained in our experiment: α activity of natural Europium provides an additional, to spontaneous fission of ^{238}U, amount of Promethium in the Earth crust at the level of 12 g; the total amount of Promethium in the whole Earth crust can be estimated as $\simeq 570$ g.

Let us finally note that the sensitivity of the present experiment was limited by the low concentration of Europium (0.4% in mass). To improve sensitivity to α activity of ^{151}Eu, one should use a detector with much higher concentration of Eu. This could be achieved, in particular, by using the $Li_6Eu(BO_3)_3$ scintillator, where concentration of Eu is two orders of magnitude higher (41%). Internal radioactive impurities of such crystals are very important in low background experiments. With this aim, some of us investigated the radioactive contamination of a sample of $Li_6Eu(BO_3)_3$ crystal in underground measurements at the Gran Sasso National Laboratories; no contaminations were found except by ^{152}Eu and ^{154}Eu [25]. Despite its rather poor scintillation properties, $Li_6Eu(BO_3)_3$ crystal might be used as low temperature scintillation bolometer, offering a good energy resolution (typically a few keV in wide energy interval) and discrimination capability between α particles and $\gamma(\beta)$ background [1,3]. The use of $Li_6Eu(BO_3)_3$ crystal as low temperature bolometer will be considered for further investigation of α decay of ^{151}Eu with higher precision.

References

[1] P. de Marcillac, et al., Nature 422 (2003) 876.
[2] F.A. Danevich, et al., Phys. Rev. C 67 (2003) 014310.
[3] C. Cozzini, et al., Phys. Rev. C 70 (2004) 064606.
[4] Yu.G. Zdesenko, et al., Nucl. Instrum. Methods A 538 (2005) 657.
[5] J.K. Bohlke, et al., J. Phys. Chem. Ref. Data 34 (2005) 57.
[6] G. Audi, A.H. Wapstra, C. Thibault, Nucl. Phys. A 729 (2003) 337.
[7] S. Agostinelli, et al., Nucl. Instrum. Methods A 506 (2003) 250;
J. Allison, et al., IEEE Trans. Nucl. Sci. 53 (2006) 270.
[8] J.B. Birks, Theory and Practice of Scintillation Counting, Pergamon, London, 1964.
[9] Yu.G. Zdesenko, et al., Nucl. Instrum. Methods A 538 (2005) 657.
[10] R. Gwin, R.B. Murray, Phys. Rev. 131 (1963) 501.
[11] D.R. Tovey, et al., Phys. Lett. B 433 (1998) 150.
[12] F.A. Danevich, et al., Phys. Lett. B 344 (1995) 72.
[13] F.A. Danevich, et al., Nucl. Phys. A 694 (2001) 375.
[14] P. Belli, et al., Nucl. Instrum. Methods A 498 (2003) 352.
[15] R.B. Firestone, et al., Table of Isotopes, eighth ed., John Wiley, New York, 1996, and CD update, 1998.
[16] E. Gatti, F. De Martini, Nuclear Electronics 2, IAEA, Vienna, 1962, p. 265.
[17] T. Fazzini, et al., Nucl. Instrum. Methods A 410 (1998) 213.
[18] L. Bardelli, et al., nucl-ex/0608004.
[19] F.A. Danevich, et al., Nucl. Instrum. Methods A 541 (2005) 583.
[20] F.A. Danevich, et al., Nucl. Instrum. Methods A 544 (2005) 553.
[21] L. Bardelli, et al., Pulse-shape discrimination with $PbWO_4$ crystal scintillators, Nucl. Instrum. Methods A, submitted for publication.
[22] O.A. Ponkratenko, V.I. Tretyak, Yu.G. Zdesenko, Phys. At. Nucl. 63 (2000) 1282;
V.I. Tretyak, in preparation.
[23] G.J. Feldman, R.D. Cousins, Phys. Rev. D 57 (1998) 3873.
[24] E. Dermateosian, L.K. Peker, Nucl. Data Sheets 66 (1992) 705.
[25] P. Belli, et al., Nucl. Instrum. Methods A 572 (2007) 734.

[26] J.K. Tuli, Nuclear Wallet Cards, Brookhaven National Laboratory, 2005.
[27] T.R. England, B.F. Rider, preprint LA-UR-94-3106.
[28] M. Attrep Jr., R.K. Kuroda, J. Inorg. Nucl. Chem. 30 (1968) 699.
[29] D.R. Lide (Ed.), CRC Handbook of Chemistry and Physics, eighty-fourth ed., CRC Press, 2003–2004, Section 14.
[30] B. Buck, A.C. Merchant, S.M. Perez, J. Phys. G 17 (1991) 1223;
B. Buck, A.C. Merchant, S.M. Perez, J. Phys. G 18 (1992) 143.
[31] D.N. Poenaru, M. Ivascu, J. Phys. 44 (1983) 791.
[32] G. Royer, J. Phys. G 26 (2000) 1149.
[33] M. Fujiwara, et al., J. Phys. G 28 (2002) 643.
[34] K. Heyde, Basic Ideas and Concepts in Nuclear Physics, IoP, Bristol, 1994.
[35] D.N. Poenaru, et al., Phys. Rev. C 32 (1985) 2198.